Hindawi
Advances in Civil Engineering
Volume 2022, Article ID 5689912, 12 pages
https://doi.org/10.1155/2022/5689912

Research Article

Experimental Study on Seismic Compression of Chinese Loess under Cyclic Direct Simple Shear Testing

Qiang Wang,[1,2] Zhe Zhang,[1] Shengjun Shao ,[2] and Qian Yang[1]

[1]*Research and Development Center for Loess Mechanics and Engineering Test Technology, Shaanxi Polytechnic Institute, Xianyang 712000, China*
[2]*Shaanxi Province Key Laboratory of Loess Mechanics and Engineering, Xi'an University of Technology, Xi'an 710048, China*

Correspondence should be addressed to Shengjun Shao; sjshao@xaut.edu.cn

Received 11 October 2021; Accepted 25 May 2022; Published 10 June 2022

Academic Editor: Wei-yao Guo

Seismic compression is the accumulation of contractive volumetric strains in unsaturated soil from earthquake shaking. For Chinese loess, the behavior of seismic compression is extremely significant and has been recognized in historical earthquakes. As a main technical mean, dynamic triaxial apparatus has been employed to study the seismic compressibility of loess for a long time. However, dynamic simple shear apparatus is superior to dynamic triaxial apparatus in modeling the real stress condition of soil under earthquake. Meanwhile, dynamic triaxial apparatus could not measure the volumetric strain of unsaturated loess precisely. A series of cyclic compression tests are hereby performed on unsaturated and intact loess by the new cyclic direct simple shear device developed in Xi'an University of Technology. The properties of cyclic compression of loess specimens are analyzed under the combined conditions of four water contents, four vertical stresses, and six shear strains. The test results reveal that the volumetric strain is constantly compacted through the process of cyclic load-unloading and is much larger during loading half-cycle than unloading half-cycle. It has been found that the cyclic compressibility of loess is dependent upon density, water content, confining pressure, shear strain (or stress), and cycles. An empirical formula to estimate the increment of cyclic volumetric strain per cycle is expressed in terms of the amplitude of shear train, dry density, water content, and vertical stress. Moreover, a simplified evaluation procedure is proposed for the probable settlements of loess deposits subjected to earthquake shaking.

1. Introduction

There is the most widespread and thickest loess in the northwest of China. The total area of loess including analogy loess reaches 640000 km^2. Furthermore, most of the area is strong seismic region as well as human settlement [1]. For most kinds of loess, void ratio is between 1.0 and 1.1, cohesive strength will decrease more than 25% once water content increases about 10%, and compressibility is prominent [2]. The particularly physical properties of loess, such as porous microstructure, weak cohesion, and rich salt, make itself show the mechanical properties of water-sensitivity, collapse, and seismic compression [3].

The seismic compression of loess has been recognized for a long time, and several settlement cases in loess site induced by earthquake or blast shock were verified and reported [4–6]. Some notable studies on the seismic compression of loess have been achieved. Zhang and Duan conducted cyclic triaxial tests on loess, found that the dynamic residual strain along the axial direction of cylindrical specimen is sizable once the amplitude of dynamic stress reaches a threshold [4]. They concluded that seismic subsidence is a special behavior of loess under earthquake load. Luo et al. considered the occurrence of seismic subsidence is owing to the collapse of soil structure when external load exceeds the structural strength of loess [7]. Zhang and Shi and Li analyzed the correlation between seismic subsidence and the types of microstructure [8, 9]. Wang et al. presented the mechanism of seismic subsidence for loess based on the changes of microstructure as seismic subsidence develops [10]. These works mainly address the generation mechanism of seismic subsidence; moreover, the methods how to evaluate the magnitude of seismic subsidence were proposed. Wang and Zhang suggested an empirical equation considering void

ratio, water content, plastic limit, liquidity index, dynamic stress, the threshold of dynamic stress of seismic subsidence, confining pressure, and number of cycles [11]. The equation includes so many physical and mechanical parameters that it is hard to deal with. Sun et al. presented a simple expression of seismic subsidence by introducing the stress ratio of equivalent stress to shear strength [12]. The physics of the equivalent stress is not definite, and the shear strength is assumed to be constant; therefore, the expression is needed to be studied furthermore.

So far, most of the present works on seismic subsidence are based on dynamic triaxial tests. The seismic subsidence of dynamic triaxial test is generally quantified using axial strain of cylindrical specimen. However, the radial strain of the cylindrical specimen in triaxial apparatus is noticeable, that is why the axial strain of cylindrical specimen is not the real volumetric strain at all. Consequently, it is not reasonable that the strain along the axial direction of cylindrical specimen is defined as seismic subsidence or compression. Generally, dynamic triaxial apparatus can be used for the dynamic liquefaction of saturated sand and the shear strength of unsaturated loess, but it is not suitable for the compressed deformation of unsaturated loess as the volumetric strain could not be measured accurately [13, 14]. Moreover, dynamic triaxial apparatus has a congenital defect that it cannot model the rotation of principal stress axis existing in soil under earthquake shake. Wong and Arthur, Symes et al., Nakata et al., and Miura et al. had verified that the principal stress rotation could produce both of shear and volumetric strains and that the effect of the principal stress rotation in the stress condition of soil under earthquake load is significant [15–18]. Comparatively, cyclic direct simple shear apparatus could model the real stress condition of soil under earthquake load better than other dynamic laboratory apparatuses.

Presented herein are a series of experimental results about seismic compression conducted on intact loess specimens by cyclic direct simple shear apparatus. The cyclic direct simple shear apparatus recently developed in Xi'an University of Technology is introduced briefly. The behavior of seismic compression of loess under different influencing factors, such as vertical stress, water content, amplitude of shear strain, and number of cycles, is analyzed. Moreover, an evaluation equation for the seismic compression of loess is proposed. The expression of seismic compress about Chinese loess, compared with the abovementioned empirical formulas, is simple and easy to use. Moreover, it should be pointed out that the magnitude of seismic compression tested in this study is much more real thanks to the approximate earthquake stress conditions simulated by cyclic direct simple shear testing. Unfortunately, all of the informed research studies are based on the testing results of dynamic triaxial apparatus, to a great extent, that is not suitable for studying seismic compress of loess.

2. Test Apparatus

The Xi'an University of Technology cyclic direct simple shear apparatus, abbreviated as XCSSA, was developed by Shao and his colleagues in 2015 [19]. The apparatus is composed mainly of microcomputer control system, hydraulic drive system, and loading mechanism. These components are shown in Figure 1. It can be seen from Figure 1 that both horizontally and vertically loading hydraulic cylinders (5) and (7) are connected with the three hydraulic cylinders (3) of the hydraulic drive system. Under the drive of step-servo motor (1), horizontal shear stress and vertical compressive stress can be applied to the cubical specimen in pressure cell (10). Both of horizontally shear displacement and force, as well as vertically compressive displacement and force, can be measured by such transducers as (6), (7), and (8).

Compared with other simple shear instruments, the XCSSA is advanced for the ingenious pressure cell, as shown in Figure 2. It can be seen from Figure 2 that the pressure cell is composed of six components, i.e., bottom platen loading along horizontal direction (2), arm of confining plate (5), rotatable and discrete confining plate that is assembled of (11), loading frame (16), top platen loading along the vertical direction (9), and top cap for the lateral confinement of top platen (8).

Figure 2 also shows that the pressure cell for cubical specimen (70∗70 mm) is surrounded with a foursquare base platen (13), two foursquare confining plates (12), two groups of rectangular parting stops (11), and a top foursquare platen (9); they are located at the underside, left and right sides, front and back sides, and upside of the specimen individually. The foursquare base platen (13), in which a porous disc is embedded, is fixed to the bottom platen (2) with four bolt bars. The arm of confining plate (5) is hinged to the bottom platen (14) and the cross beams of confining plates (10) via four hinge joints in the same way. The hinged joint enables not only the connection but also the rotation between the components (2), (5), and (10). The hinged joints at downside can only move along the slide guide (1), while at upside can only move along the slide guide (6), as shown in Figure 2. The top platen (9) is composed of a foursquare plate and a loading shaft, of which the former is installed on the upside of the cubical specimen, and the latter passing the top cap (8) is connected with the hydraulic cylinder along vertical direction. Then, when the top cap (8) is fixed to loading frame (16), the top platen can only move along the vertical direction. Thereby, the cubical space of pressure cell could shape into a rhombohedral one when the bottom platen moves forward or backward, and the top platen moves up and down accordingly. The change of rhombohedral space from cubical space exerts uniform shear deformation on the cubical specimen under lateral confinement, and the according movement of top platen actualizes the continuity of volume deformation.

3. Specimen Preparation and Testing Conditions

The specimens for cyclic simple shear test are sampled from a flat loess site, located at the suburban district of Xi'an City. The depth of sample is about 7 m, and the corresponding layer was deposited in the Upper Quaternary. In order to obtain undisturbed samples at depth of 7 m, several circular pits (diameter = 1.2 m) are excavated by hand and power equipment. By virtue of the high strength of loess under low

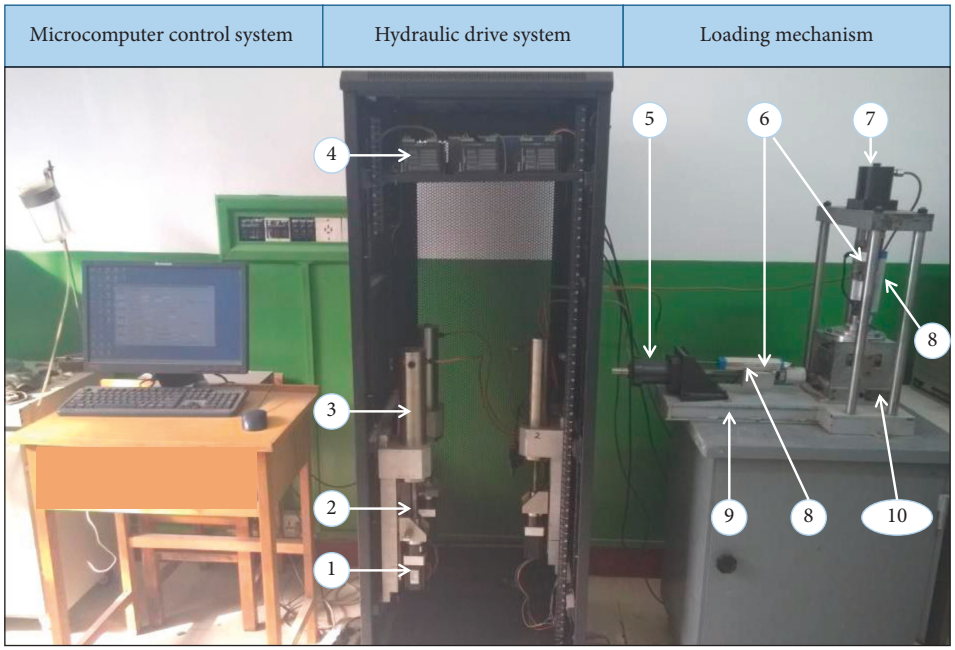

Figure 1: Components of XCSSA: step-servo motor (1), ball screw (2), hydraulic cylinder (3), single-chip microcomputer (4), horizontally-loading hydraulic cylinder (5), pressure transducer (6), vertically loading hydraulic cylinder (7), displacement transducer (8), reaction base (9), and pressure cell (10).

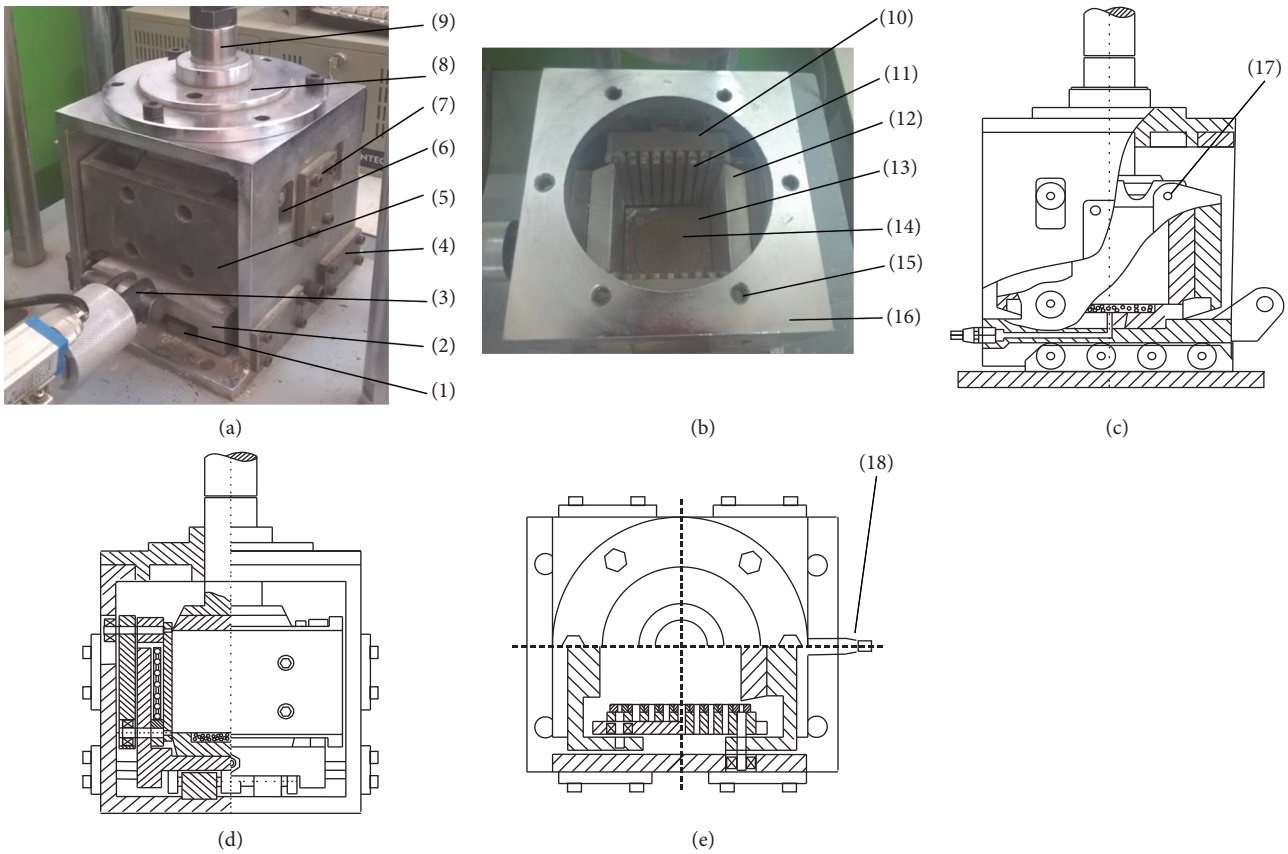

Figure 2: General view (a), top views (b, e), and lateral views (c, d) of pressure cell: horizontal guide (1), bottom platen (2), connecting link (3), support for confining roller (4), arm of confining plate (5), vertical guide (6), support for confining roller of cross beam (7), top cap (8), top platen (9), cross beam (10), rectangular parting stop (11), confining plate (12), base plate for specimen (13), porous stone (14), bolt hole (15), loading frame (16), hinged hole (17), and drainage hole (18).

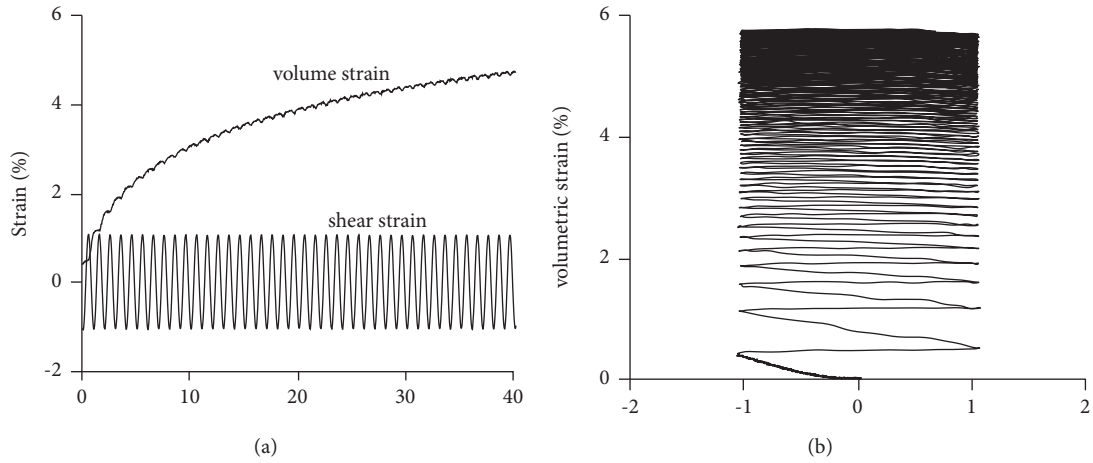

Figure 3: Typical curves of shear and volumetric strains for loess under cyclic direct simple shearing. (a) Number of cycles. (b) Shear strain.

water content, the side wall of test pit is commonly stable and safe, i.e., personal can access the test pit without support measures. Several tens of meters high loess cliff and loess cave to dwell are examples for the stability of dry loess. Herein, personal accesses the test pit for sampling by hand when the pit is dug to the depth of 8 m. Then, large block of samples can be cut from the sidewall of test pit at depth of 7 m. In this way, an enormous amount of 30~40 cm cubical samples at the same depth is gotten, sealed, and carried to the laboratory. Finally, the massive sample is trimmed to several 7 cm cubical specimens by a special sample cutter matching the cyclic simple shear apparatus. The physical parameters of the natural loess are listed as follows: natural density = 1.54~1.55 g/cm3, dry density = 1.35~1.36, water content = 13%~15%, void ratio = 0.98~1.05, liquid limit = 35%, plastic limit = 22%, and specific gravity of grain = 2.7.

By the apparatus, a series of cyclic direct simple shear tests with different test conditions of consolidation pressure, water content, and amplitude of shear strain are conducted on intact loess specimens under full drainage. In all, 96 loess specimens are tested under the combined conditions of one kind of load, i.e., strain controlled sinusoid wave, four water contents = 5%, 10%, 15%, and 20%, four consolidation pressures = 50, 100, 150, and 200 kPa, and six amplitudes of shear strain = 0.15%, 0.5%, 1.0%, 2.0%, 3.0%, and 4.5%. The loess specimens tested here are sampled from the same depth of the same site, thus can be considered as the same kind with the same fabric and dry density. Different water contents of 5%, 10%, 15%, and 20% can be prepared by air drying or water permeating on natural loess according to natural water content. The other test conditions can be carried on specimens by apparatus directly.

4. Behavior of Seismic Compression of Loess

Figure 3 demonstrates the typical test results of the cyclic compression on loess specimen under water content = 15%, consolidation pressure = 150 kPa, and amplitude of shear strain = 1%. It can be seen from Figure 3(a) that owing to the cyclic excitement of shear strain on loess specimen, a progressively incremental volumetric strain generates. The increment of volumetric strain becomes smaller and smaller as the total volumetric strain increases. The test results show that for loess the arrangement of soil particles becomes condensed because of the cyclic shear strain and vertical stress. When the applied shear strain excesses the threshold shear strain, the initial microstructure of loess should be destroyed. Then, accompanying with the vertical stress, soil particles might rearrange to update stability conditions, and the void between soil particles will decrease. Figure 3(b) also shows that the magnitude of volumetric strain has the distinct directional property that volumetric strain generated during the loading direction is much larger than that during the unloading direction and that volumetric strain is compacted no matter what kind of loading direction is applied.

4.1. Effect of the Amplitude on Shear Strain. Figure 4 displays the time histories of volumetric strain versus the number of cycles for loess specimens under different amplitudes of shear strain, water contents, and vertical stresses. Figures 4(a) to 4(d) demonstrate the influence of shear strain on volumetric strain for loess under different water contents and vertical stresses. It is obvious in Figure 4 that the magnitude of volumetric strain has a positive correlation with the amplitude of volumetric strain and the number of cycles. This testing phenomenon can be observed for loess specimens under whatever test conditions are, as well as the dry sand [20]. The larger amplitude of shear strain is, the more serious damage loess undergoes. Correspondingly, the damaged microstructure of loess cannot support the initial vertical stress, and the larger soil particles lie down and the smaller particles fill in the void between soil particles. Thereupon, the loess becomes much more compacted once undergoes the larger amplitude of shear strain.

4.2. Couple Effects of Vertical Stress and Water Content. Figure 5 shows the influence of vertical stress on volumetric strain history under two water contents of 5% and 20%. From Figures 5(a) and 5(b) as water content equals 5%, it can

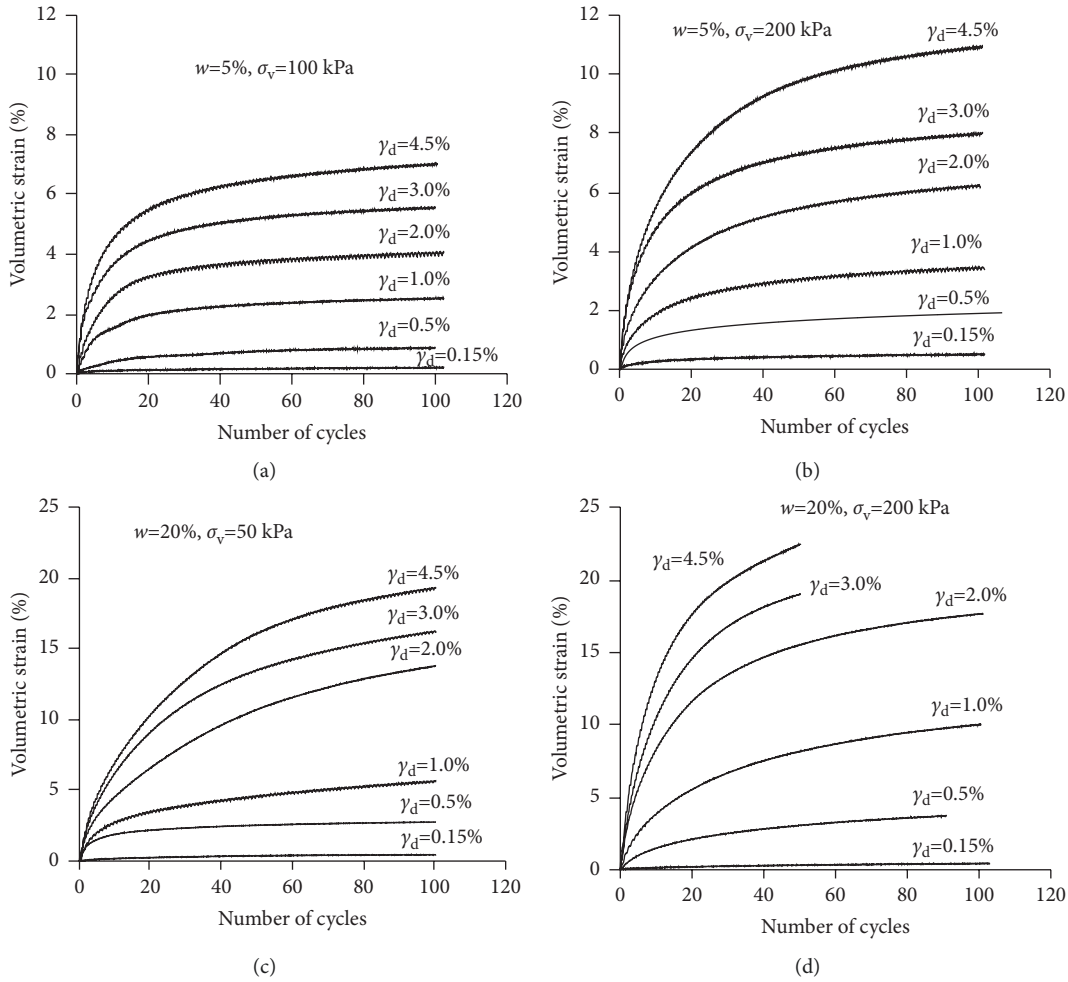

Figure 4: Comparison between the volumetric strain time histories under different amplitudes of shear strain (here, w is water content, σv is vertical stress, and γd is the amplitude of shear strain).

be observed that the bigger vertical stress is, the much more rapidly cyclic volumetric strain increases. While for loess under water content = 20%, Figure 5(c) shows the history curves of volumetric strain during the vertical stresses of 150 and 200 kPa are distributed the underside of that under the vertical stresses of 50 and 100 kPa, and Figure 5(d) displays both history curves under the vertical stresses of 150 and 200 kPa coincide almost. The difference of the effect of vertical stress on volumetric strain under low and high water contents reveals the double actions of confining pressure. On one hand, loess would yield and generate plastic volumetric strain as confining pressure increases; on the other hand, the shear strength and stiffness of loess might be reinforced thinks to the hydrostatic stress of confining pressure.

As an especially structural and water-sensitive soil, loess commonly has very obvious compressive yield strength, and the strength is highly sensitive to water. When water content is low, the strength of loess is comparatively large. However, the strength will decrease very significantly once water immerses loess, as shown in Figure 6. Look back on Figures 5(c) and 5(d), when loess specimen undergoes the vertical stresses of 150 and 200 kPa, significant consolidation deformation generates before the excitation of cyclic loading, because the vertical stresses 150 and 200 kPa are larger than the yield strength of water content = 20% loess. The consolidation deformation restraints the further development of volumetric strain, which is apparent for loess under little amplitude of shear strain rather than large one, as shown in Figure 5(c).

The humidification of loess could cause the connecting strength between soil particles decreased because of the diminution of water film and the dissolution of cementitious minerals. Therefore, water is commonly a trigger for the settlement of loess site. It is verified that the seismic volumetric strain of loess increases with the increment of water, seen in Figure 7.

5. Empirical Equation for the Seismic Compression of Loess

As analyzed above, for a certain loess the seismic volumetric strain ε_v is related to the amplitude of shear strain γ_d, number of cycles N, vertical stress σ_v, and water content w. Moreover, the seismic volumetric strain must be dependent on initial dry density ρ_d, which represents the potential of

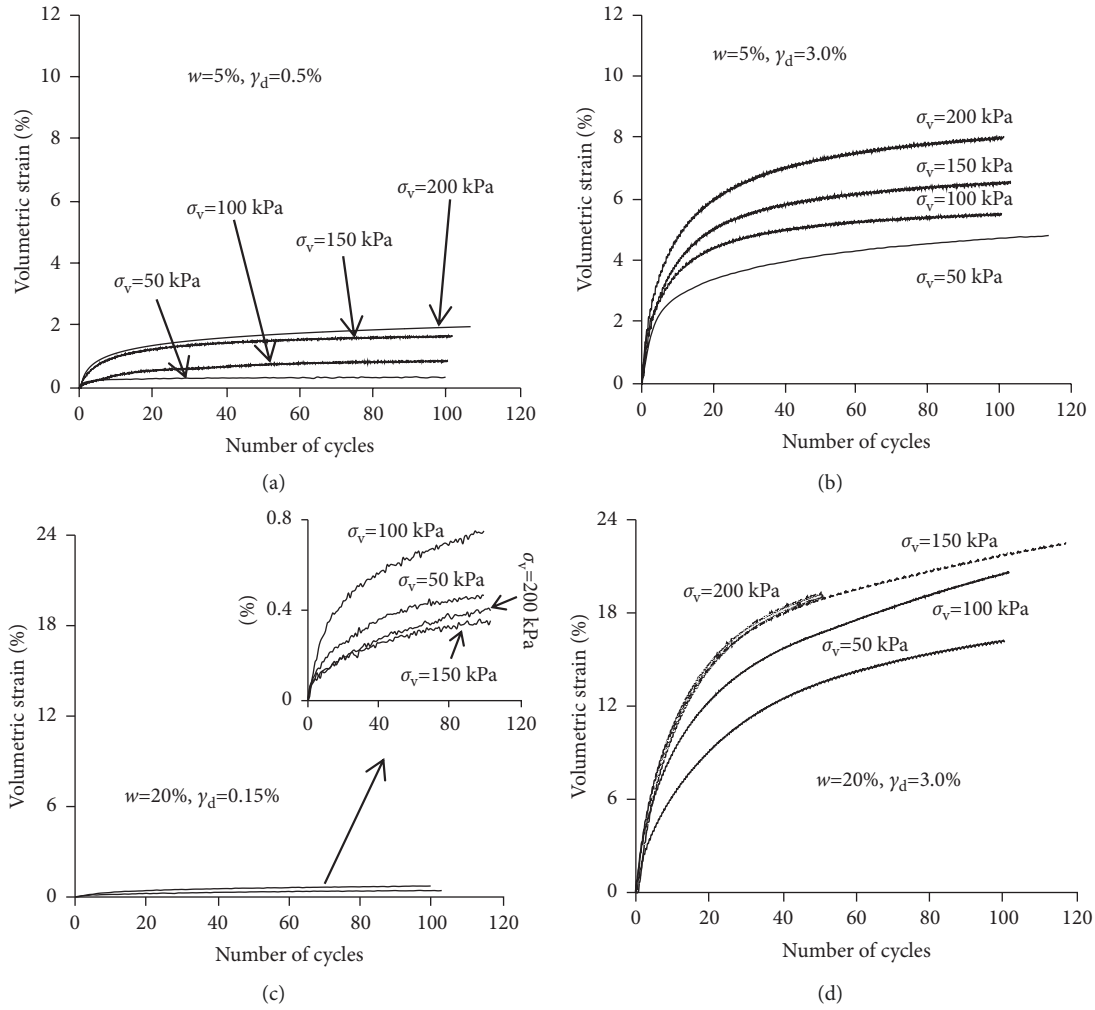

Figure 5: Comparison between the volumetric strain time histories under different vertical stress (here, w is water content, σv is vertical stress, and γd is the amplitude of shear strain).

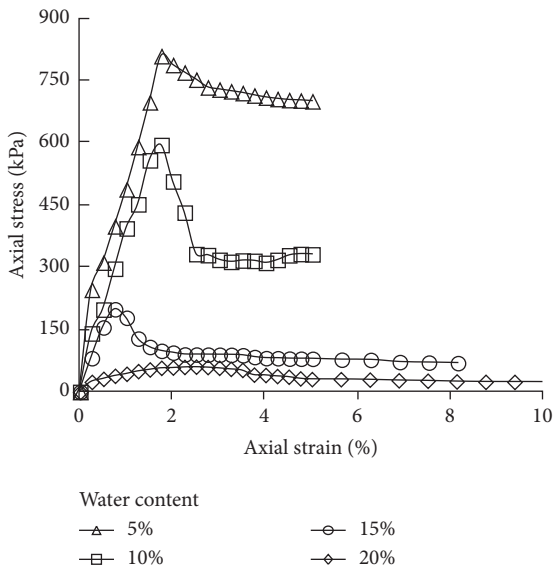

Figure 6: Stress-strain curves of intact loess under different water contents.

compressibility. Then, the seismic volumetric strain can be expressed as equation (1), the increment of seismic volumetric strain $\nabla\varepsilon_v$, i.e., the seismic volumetric strain per the cycle of strain, can be expressed by

$$\varepsilon_v = F(\gamma_d, N, \sigma_v, w, \rho_d), \tag{1}$$

$$\nabla\varepsilon_v = Q(\gamma_d, \varepsilon_v, \sigma_v, w, \rho_d). \tag{2}$$

5.1. Cyclic Shear-Volume Coupling Equation. For sand under cyclic simple shearing, Martin et al. proposed an incremental shear-volume coupling equation according to the relationship between ε_v and $\nabla\varepsilon_v$ under different γ_d [20]. The equation involves four parameters resulting in hard to use. Hence, Byrne analyzed the normalized $\varepsilon_v/\gamma_d - \nabla\varepsilon_v/\gamma_d$ relationship and presented a simplified two-parameter equation (3) based on the same concepts as in the Martin model [21]. In the same way, the $\varepsilon_v/\gamma_d - \nabla\varepsilon_v/\gamma_d$ relationship scatter diagrams of loess under several different test conditions are plotted in Figure 8. It can be seen from Figure 8 that all data

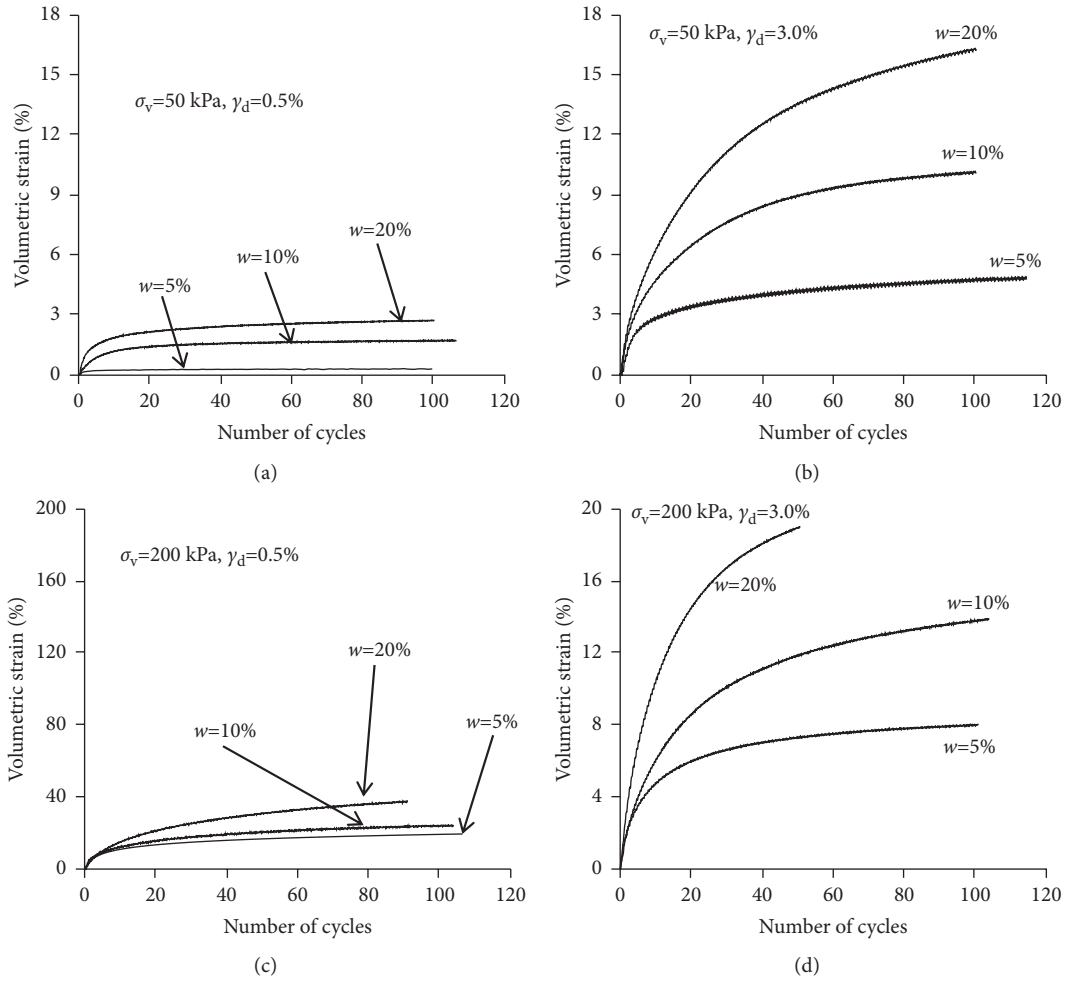

Figure 7: Stress-strain curves of intact loess under different water contents.

points are distributed along a smooth curve that can be well represented by equation (3). Similarly, the other experimental test data that are not shown in this paper have the same law as illustrated in Figure 8:

$$\Delta\varepsilon_v/\gamma_d = a \cdot \exp\left(-b \cdot \varepsilon_v/\gamma_d\right), \tag{3}$$

where a and b are constants for the loess in question at the water content, vertical tress, and dry density under consideration.

According to equation (3), the increment of volumetric strain is positively correlated to a, while negative with b. When $\varepsilon_v = 0$, a equals the ratio of the first cyclic volumetric strain to the amplitude of shear strain, i.e., $(\nabla\varepsilon_v)$ cycle1$/\gamma_d$. The parameter a controls the magnitude of volume change, while b controls the shape of the accumulated volume change with the development of total volumetric strain.

5.2. Cyclic Shear-Volume Coupling Equation Incorporating Initial Dry Density. It has been noted that the parameters a and b can be expressed in terms of water content w, vertical stress σ_v and dry density ρ_d, although dry density is not taken into consideration by the tests. In the process of cyclic volume change, the dry density of loess specimen changes all the time; in the other words, the loess specimen at any moment can be considered as another loess specimen with different dry density. Therefore, the same kind of loess would conform the same $\varepsilon_v/\gamma_d - \nabla\varepsilon_v/\gamma_d$ relationship, even though the initial density is different. Then, when the initial dry density ρ_d^0 is larger or smaller than the reference dry density ρ_d^{ref}, the corresponding loess is called seismically overcompressed or undercompressed loess with respect to reference loess. They are identified by points A, B, and C in Figure 9 and conform the same equation as

$$\frac{\Delta\varepsilon_v}{\gamma_d} = a \cdot \exp\left(\frac{-b\left(\varepsilon_v + \rho_d^{ref} - \rho_d^0/\rho_d^0\right)}{\gamma_d}\right), \tag{4}$$

where the parameters a and b are determined by reference loess.

5.3. Empirical Expression of a and b Values. For the same kind of loess, once initial dry density is considered as reference dry density, the parameters a and b should be dependent on the vertical stress σ_v and the water content w

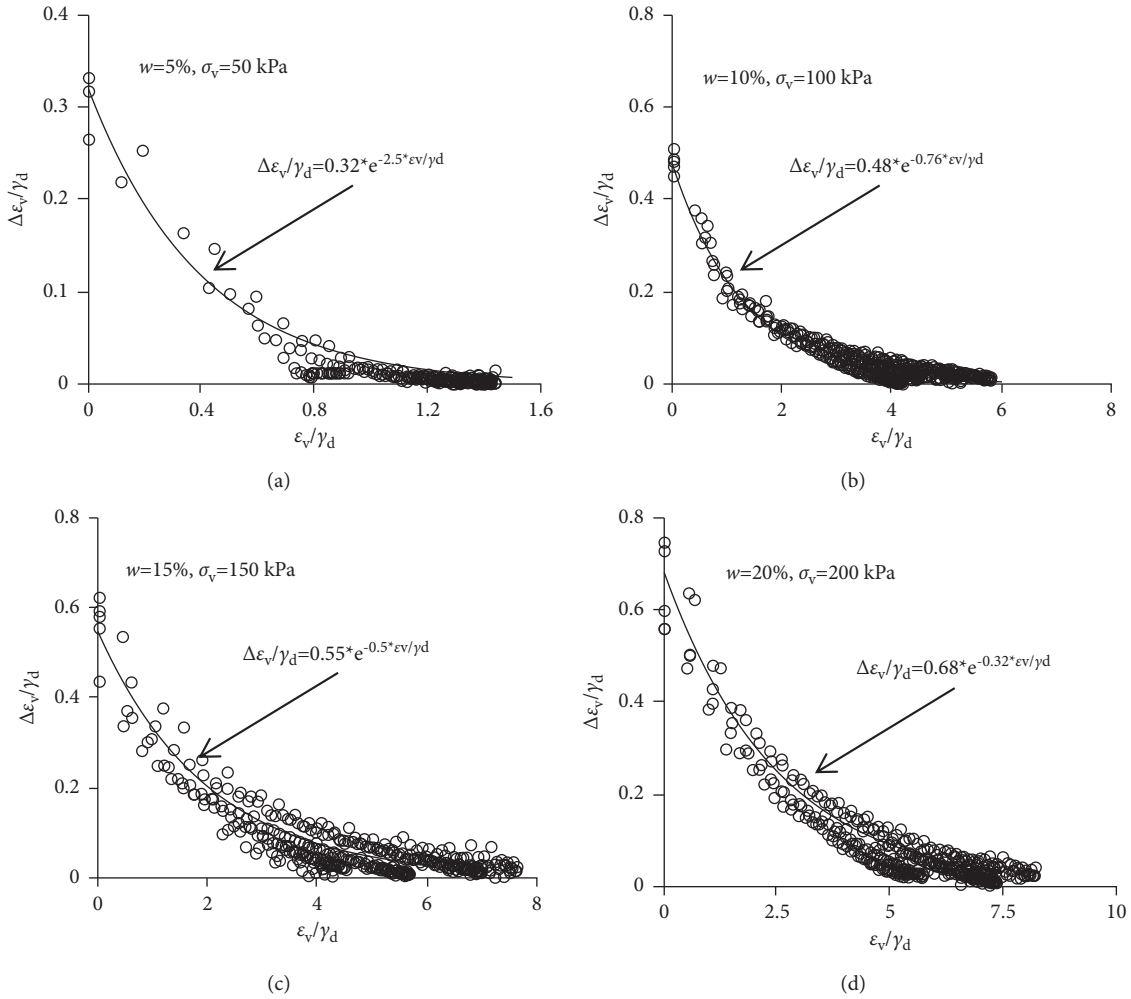

Figure 8: $\varepsilon_v/\gamma_d - \nabla\varepsilon_v/\gamma_d$ scatter diagrams of loess under several test conditions.

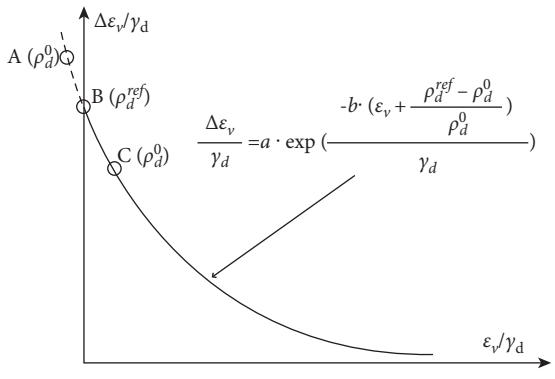

Figure 9: $\varepsilon_v/\gamma_d - \nabla\varepsilon_v/\gamma_d$ curve considering dry density.

only. Then, both a and b can be a function of σ_v and w, respectively. According to the cyclic simple shear test data, the same as Figure 8, the correspondence of a (or b) with σ_v and w can be obtained. Furthermore, the corresponding relationships of a (or b) and σ_v during $w = 5\%$, 10%, 15%, and 20% can be deduced, as shown in Figure 10. It can be seen from Figure 10 that both a and b are linear with σ_v. Values of a increases, while b decreases with the larger σ_v. The relationships are consistent with the effect of vertical stress on the cyclic compression of loess. From Figure 10, we can see that a and b can be written by the form of

$$\begin{cases} a = \alpha\sigma_v + \beta \\ b = \omega\sigma_v + \psi. \end{cases} \tag{5}$$

The parameters α, β, ω, and ψ in equation (5) are changing with water content, which is visible by comparing Figures 10(a)–10(d). The changes reflect the couple effect of vertical stress and water content on the behavior of cyclic compression of loess. Furthermore, the changing law of parameters α, β, ω, and ψ with water content w is illustrated in Figure 11. Seen from Figure 11, α is a constant independent of water content, while β, ω, and ψ are linear with water content. The relations are written as

$$\begin{cases} \alpha = 0.0021 \\ \beta = 0.95w + 0.131 \\ \omega = 0.068w - 0.014 \\ \psi = -17.8w + 3.806. \end{cases} \tag{6}$$

Substituting the above equations in equation (5) leads to

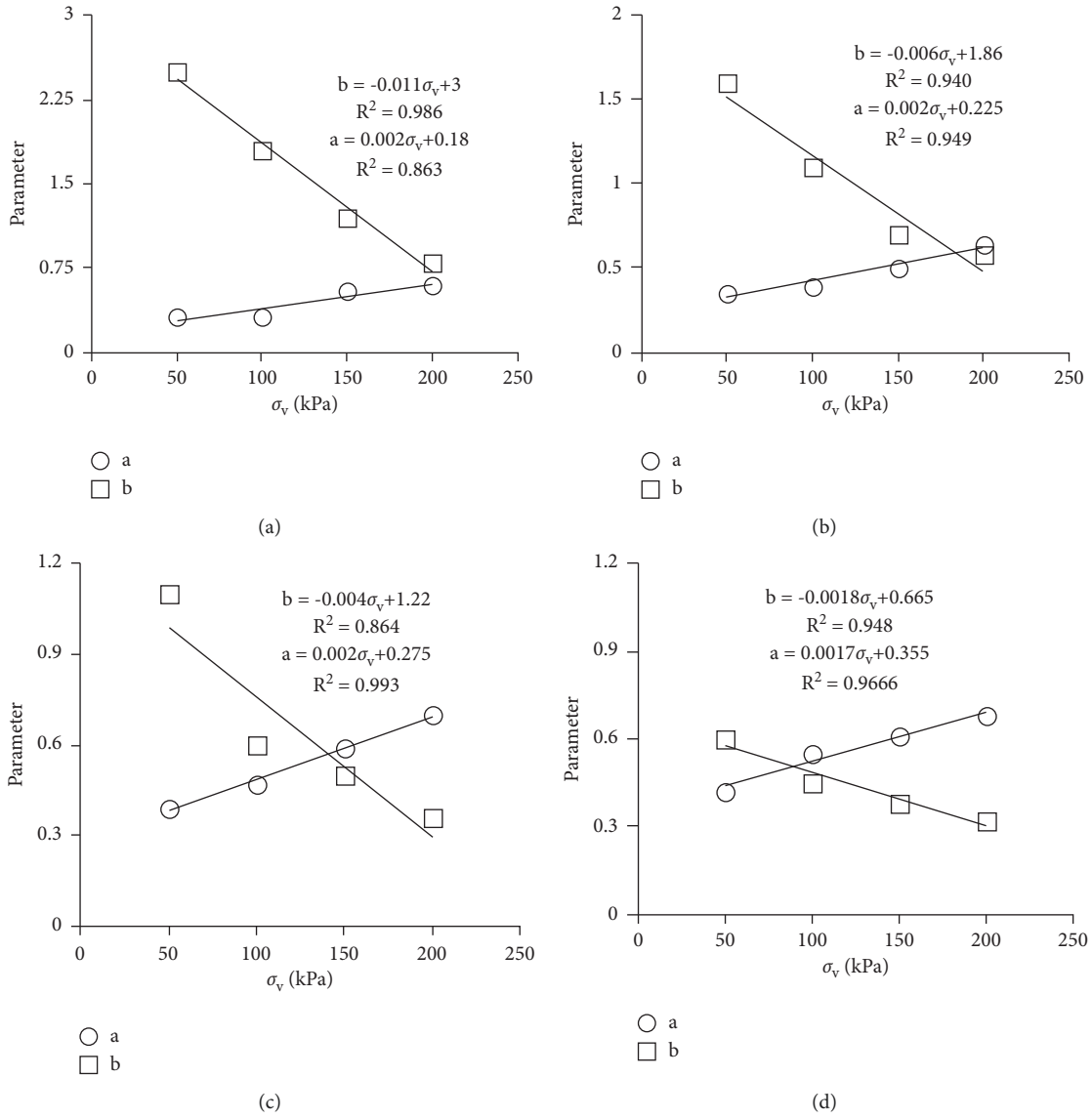

Figure 10: Parameters a and b versus vertical stress under different water contents (a) =5%, (b) =10%, (c) =15%, and (d) =20%.

$$\begin{cases} a = 0.21\dfrac{\sigma_v}{P_a} + 0.95w + 0.131, \\ b = 6.8w\dfrac{\sigma_v}{P_a} - 1.4\dfrac{\sigma_v}{P_a} - 17.8w + 3.806, \end{cases} \quad (7)$$

where as both a and b are dimensionless material parameters, Pa is the atmospheric pressure that is used in the formulation to eliminate unit system selection effect.

6. Consideration on the Empirical Model Application

The empirical model is based on the experimental data of Xi'an loess with the water content 5%~20%, the vertical stress 50~200 kPa, and the amplitude of shear strain 0.15%~4.5%. Even so, the model reveals and conforms the influence function of water content, vertical stress, shear strain, and cycles on the cyclic volumetric strain of loess considerably. Moreover, 5%~20% is the ordinary natural water content of loess, and especially, the loess with water content <5% does not exist nearly; the depth of loess corresponding to the vertical stress 50~200 kPa is about from 4.5 m to 18 m, which corresponds to the main layer of seismic compression needs to be concerned. Also, it has been confirmed that the effect of vertical stress might be neglected when water content >20% and vertical stress >200 kPa, while is notable when water content is smaller. On the other hand, it may be considered that volumetric strain of soil cannot be caused by shear strain if confining pressure =0. Then, the parameter a, representing the volumetric strain after the first cycle, might be zero as $\sigma_v = 0$, and b would be an infinitely large quantity; here is 100. Correspondingly, the parameters a and b might be estimated by the interpolation method during $\sigma_v = 0$~50 kPa. Hence, the values for a and b are assumed to obey:

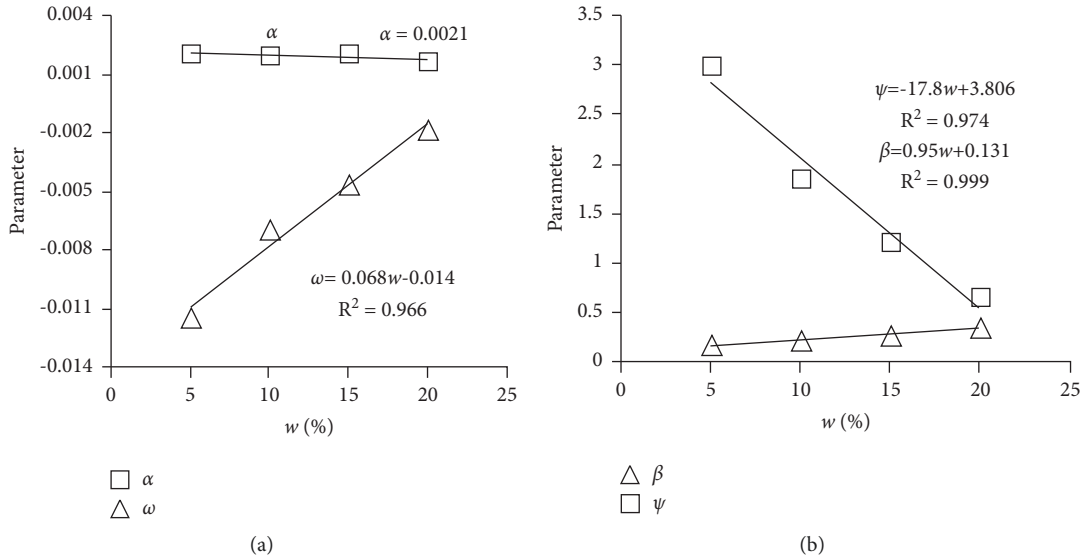

Figure 11: Parameters α, β, ω, and ψ versus water content.

Table 1: Equivalent cycles versus earthquake magnitude.

Earthquake magnitude	Number of representative cycles at $0.65a_{max}$	Earthquake duration (s)
5.5~6.0	5	8
6.5	8	14
7.0	12	20
7.5	20	40
8.0	30	60

(a) $\sigma_v = 200$ kPa when σ_v and w are larger than 200 kPa and 20%, respectively, then

$$\begin{cases} a = 0.95w + 0.551, \\ b = -4.2w + 1.006. \end{cases} \quad (8)$$

(b) When it is between 0 and 50 kPa,

$$\begin{cases} a = \dfrac{2\sigma_v}{P_a}(0.95w + 0.236) \\ \\ b = 100 - \dfrac{\sigma_v}{P_a}(193.8 + 28.8w). \end{cases} \quad (9)$$

(c) Equation (7) for other conditions.

According to equations (4) and (7) ~ (9), the cyclic volumetric strain corresponding to any given cycles can be calculated. The calculation needs to determine such physical conditions of loess as w and ρ_d^0, the static stress condition of σ_v, and the cyclic loading conditions of γ_d and n. Generally, w and ρ_d^0 are the fundamental physical indexes provided in geotechnical investigation report and can be easily tested. Moreover, the vertical stress at any given depth can be easily computed with w and ρ_d^0. On the other hand, γ_d, i.e., effective shear strain γ_{eff}, may be estimated by equation (10) presented by Tokimatsu and Seed [22], and n might be computed according to the relationship between equivalent cycles and earthquake magnitude, seen in Table 1 proposed by Seed et al. [23]. This procedure is not as accurate as performing a dynamic response analysis, but it is probably accurate enough for most settlement estimates in practice:

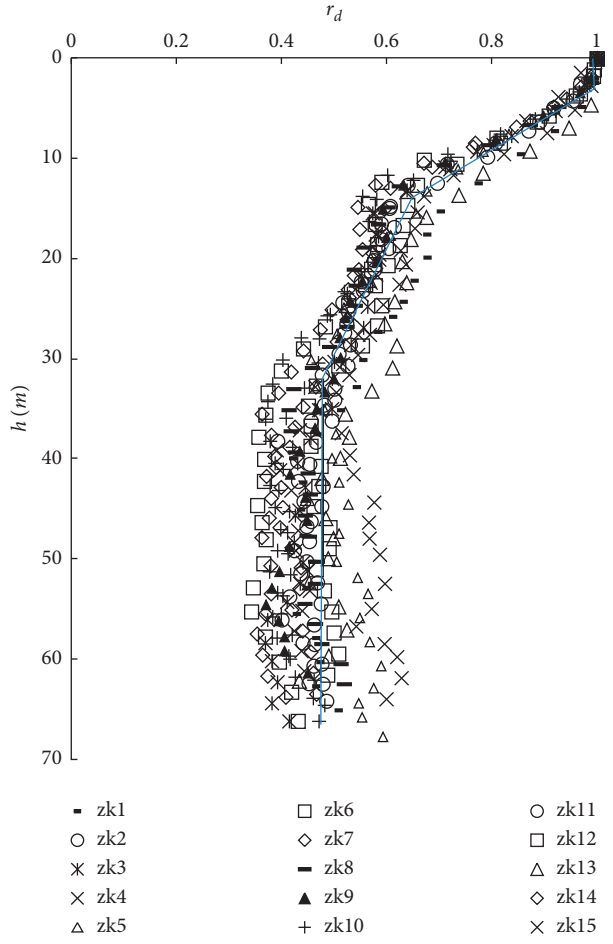

Figure 12: Shear stress reduction versus depth for loess site.

$$\gamma_{\text{eff}}\frac{G_{\text{eff}}}{G_{\max}} = \frac{0.65 \cdot a_{\max} \cdot \sigma_0 \cdot r_d}{g \cdot G_{\max}}, \tag{10}$$

in which G_{eff} = effective shear modulus at induced strain level; $G_{\max}$ = shear module at low stain level; $a_{\max}$ = maximum horizontal acceleration at the ground surface; σ_0 = total overburden pressure at the depth considered; and r_d = shear stress reduction factor, which can be given by a considerable computations in Figure 12 as

$$r_d(h) = \begin{cases} 1, & 0 \le h < 3, \\ \dfrac{(34.429 - h)}{31.429}, & 3 \le h < 14, \\ \dfrac{(82.824 - h)}{105.88}, & 14 \le h < 32, \\ 0.48, & 32 \le h, \end{cases} \tag{11}$$

where h is depth.

7. Conclusion

The magnitude of compression is noticeable for the Chinese loess under cyclic shear loading. The volumetric strain is constantly compacted through the process of cyclic load-unloading and is much larger during loading half-cycle than unloading half-cycle. The cyclic direct simple shear tests illustrate that the cyclic compression of loess is dependent upon density, water content, confining pressure, shear strain (or stress), and cycles. As the same as dry sand, the relationship between the increment of volumetric strain per cycle and accumulated volumetric strain, once normalized by the amplitude of shear strain, might be fitted with the same curve regardless of the amplitude of shear strain. The fitting curves for loess under different water content and vertical stress may be represented with the same formula including two parameters, which can be estimated with water content and vertical stress.

In the final analysis, the cyclic shear-volume coupling equation proposed here is an empirical formula and therefore could not express the physical mechanics of seismic compression of loess. For this reason, the cyclic shear-volume coupling equation and its parameters can be only applied to some kinds of loess rather than other soils. However, a simplified evaluation procedure has been proposed for the probable settlements of loess deposits subjected to earthquake shaking. The approach might be applicable to estimate the objectives whose amount is huge but accuracy requirement is not high, although the procedure is not as accuracy as dynamic response analysis. The proposed approach needs further works to verify its practicability and inaccuracy.

Data Availability

All the data included in this study are available upon request by contact with the corresponding author.

Conflicts of Interest

The authors declare that they have no conflicts of interest.

Acknowledgments

This work was sponsored by the Research and Development Center for Loess Mechanics and Engineering Test Technology of Shaanxi Polytechnic Institute, the Doctoral Fund of Shaanxi Polytechnic Institute (no. BSJ 2021-08) and the National Natural Science Foundation of China (no. 52178355).

References

[1] L. Wang, *Loess Dynamics*, Earthquake Press, Beijing, 2003.
[2] S. Chang and S. Zhang, *Engineering Geology Manual*, China Architecture & Building Press, Beijing, 2007.
[3] D. Xie, "Exploration of some new tendencies in research of loess soil mechanics," *Chinese Journal of Geotechnical Engineering*, vol. 23, no. 1, pp. 3–13, 2001.
[4] Z. Zhang and R. Duan, "Discussion on seismic subsidence of loess sites in the northwest of China during Earthquake," in *Proceedings of the International Symposium on Engineering Geology Problems in Seismic Areas*, pp. 65–76, Bari, October 1986.
[5] Q. Wang, S. Shao, J. Wang, and Z. Zhang, "Review on disaster characteristics of the seismic subsidence of loess site and its formation causes," *Journal of Seismological Research*, vol. 39, no. 4, pp. 692–702, 2016.
[6] L. Wang, J. Sun, X. Huang et al., "A field testing study on negative skin friction along piles induced by seismic subsidence of loess," *Soil Dynamics and Earthquake Engineering*, vol. 31, no. 1, pp. 45–58, 2011.
[7] Y. Luo, D. Xie, W. Dong, and C. Chen, "Comparative analysis of the vibration deformation behavior of the loess from the different regions," *Journal of Shaanxi Water Power*, vol. 17, no. 1, pp. 4–7, 2001.
[8] Z. Zhang, *Predication of Earthquake Disasters in Loess Area*, Earthquake Press, Beijing, 1999.
[9] Y. Shi and L. Li, "Micro-analysis on seismic subsidence characteristics of loess," *Chinese Journal of Rock Mechanics and Engineering*, vol. 22, no. 2, pp. 2829–2833, 2003.
[10] L. Wang, J. Deng, and Y. Huang, "Quantitative analysis of microstructure of loess," *Chinese Journal of Rock Mechanics and Engineering*, vol. 26, no. 1, pp. 3025–3031, 2007.
[11] L. Wang and Z. Zhang, "A method of estimating the quantity of seismic subsidence in loess deposits during earthquake," *Journal of Natural Disasters*, vol. 2, no. 3, pp. 85–94, 1993.
[12] J. Sun, S. Xu, L. Wang, J. Wang, and W. Tian, "Critical influence parameters and magnitude estimation of dynamic residual strain of unsaturated loess," *Chinese Journal of Rock Mechanics and Engineering*, vol. 31, no. 2, pp. 382–391, 2012.
[13] M. L. Silver, F. Tastsuoka, A. Phukunhaphan, and A. S. Avramidis, "Cyclic undrained strength of sand by triaxial test and simple shear test," in *Proceedings of the 7th World Conference on Earthquake Engineering*, pp. 281–288, Istanbul, Turkey, October 1980.
[14] G. Gao, C. Nie, and X. Gu, "A review of recent research in laboratory test of seismic compression of sands," *Advances in Science and Technology of Water Resources*, vol. 36, no. 6, pp. 1–7, 2016.

[15] R. K. S. Wong and J. R. F. Arthur, "Sand sheared by stresses with cyclic variations in direction," *Géotechnique*, vol. 36, no. 2, pp. 215–226, 1986.

[16] M. J. Symes, A. Gens, and D. W. Hight, "Drained principal stress rotation in saturated sand," *Géotechnique*, vol. 38, no. 1, pp. 59–81, 1988.

[17] Y. Nakata, M. Hyodo, H. Murata, and N. Yasufuku, "Flow deformation of sands subjected to principal stress rotation," *Soils and Foundations*, vol. 38, no. 2, pp. 115–128, 1998.

[18] K. Miura, S. Miura, and S. Toki, "Deformation behavior of anisotropic dense sand under principal stress axes rotation," *Soils and Foundations*, vol. 26, no. 1, pp. 36–52, 1986.

[19] S. Shao, Q. Wang, and S. Shao, "Development of a new cyclic simple shear apparatus and test verification on loess," in *Proceedings of the 6th Asia Pacific Conference on Unsaturated Soils*, pp. 257–261, Guilin, November 2015.

[20] G. R. Martin, H. B. Seed, and W. D. L. Finn, "Fundamentals of liquefaction under cyclic loading," *Journal of the Geotechnical Engineering Division*, vol. 101, no. 5, pp. 423–438, 1975.

[21] P. M. Byrne, "A cyclic shear-volume coupling and pore pressure model for sand," in *Proceedings of the Second International Conference on Recent Advances in Geotechnical Earthquake Engineering and Soil Dynamics*, pp. 47–55, Rolla, Feb 1991.

[22] K. Tokimatsu and H. B. Seed, "Evaluation of settlements in sands Due to earthquake shaking," *Journal of Geotechnical Engineering*, vol. 113, no. 8, pp. 861–878, 1987.

[23] H. B. Seed, I. M. Idriss, F. Makdisi, and N. Banerjee, "Representation of irregular stress time histories by equivalent uniform stress series in liquefaction analysis," in *Earthquake Engineering Research Center*University of California, Berkeley, 1975.